New Journal of Physics
The open access journal at the forefront of physics

Deutsche Physikalische Gesellschaft DPG IOP Institute of Physics

PAPER • OPEN ACCESS

Experimental verification of the Landau–Lifshitz equation

To cite this article: C F Nielsen *et al* 2021 *New J. Phys.* **23** 085001

New Journal of Physics
The open access journal at the forefront of physics

Deutsche Physikalische Gesellschaft DPG
IOP Institute of Physics

Published in partnership with: Deutsche Physikalische Gesellschaft and the Institute of Physics

OPEN ACCESS

RECEIVED
8 June 2021

REVISED
12 July 2021

ACCEPTED FOR PUBLICATION
16 July 2021

PUBLISHED
3 August 2021

PAPER

Experimental verification of the Landau–Lifshitz equation

C F Nielsen[1,*], J B Justesen[1], A H Sørensen[1], U I Uggerhøj[1], R Holtzapple[2] and CERN NA63

[1] Department of Physics and Astronomy, Aarhus University, 8000 Aarhus, Denmark
[2] Department of Physics, California Polytechnic State University, San Luis Obispo, CA 93407, United States of America
[*] Author to whom any correspondence should be addressed.

E-mail: christianfn@phys.au.dk

Keywords: radiation reaction, strong fields, classical electrodynamics

Abstract

The Landau–Lifshitz (LL) equation has been proposed as the classical equation to describe the dynamics of a charged particle in a strong electromagnetic field when influenced by radiation reaction. Until recently, there has been no clear experimental verification. However, aligned crystals have remedied the situation: here, as in Nielsen *et al* CERN NA63 Collaboration (2020 *Phys. Rev. D* **102** 052004), we report on a quantitative experimental test of the LL equation by measuring the emission spectra of electrons and positrons penetrating aligned single crystals. The recorded spectra are in remarkable agreement with simulations based on the LL equation of motion with moderate quantum corrections for recoil and, in the case of electrons in axially aligned crystals, spin and reduced radiation intensity.

1. Introduction

Under typical experimental conditions the energy radiated by an accelerated charged particle is negligible compared to its kinetic energy. The radiation can then be safely neglected in determining the dynamics of the particle. However, if the particle undergoes sufficiently large accelerations, this is no longer true. In this case it is essential to include the back-action of the radiation, called the radiation reaction [2–6]. Such large accelerations, due to strong external electromagnetic fields, are present in the focal-points of lasers of sufficiently high power, but are also achievable for ultrarelativistic particles penetrating oriented single crystals. In this paper we report on recent experimental investigations of radiation reaction in single crystals. The article presents a condensed version of the main results in [1] emphasizing physics pertinent to the expected audience of the special issue in hand. We begin with a short overview of studies of strong-field effects in crystals over the last four decades and their connection to strong-field laser studies.

2. Strong-field effects in crystals

Strong field effects in quantum electrodynamics have been studied extensively in experiments, utilizing the intense electric fields in crystals combined with electrons of very high Lorentz factors, starting in the early 1980's with a series of theoretical papers by Baryshevskii and Thikhomirov [7–10] and the independent theoretical study by Kimball *et al* [11]. Since then, a number of increasingly detailed experiments have been performed employing strong crystalline fields. The first experiments confirmed, with relatively low statistics, the strong field behaviors of the enhancement of pair creation and radiation emission [12–14] averaged over large slices in energy and incident angle. It was shown that photons incident along a crystal axis will pair produce in the strong field with a higher probability than that of an amorphous target, and that the spectrum differential in the positron energy is completely different. The first observation of quantum recoil effects in synchrotron radiation from strong fields appeared from an experiment performed at SLAC, where a collimated beam of 4, 15 and 17.5 GeV positrons was directed along the ⟨100⟩ axis of a diamond crystal. The results confirmed the newly developed theory [15, 16] treating the strong-field radiation emission similar to synchrotron radiation by dividing the particle trajectory into nearly circular segments and

summing the appropriately weighted contributions. Even at the comparatively low values of the strong-field parameter, a significant suppression of the radiation yield compared to the classically calculated value resulted. A few years later, the 'Belkacem peak' was discovered [17] by sending 150 GeV electrons through a thin axial aligned Ge crystal resulting in an enhancement of radiation yield sharply peaked at photon energies of about 85% of the electron energy. The experiment showed an enhancement, the increase of the crystalline case compared to an otherwise equivalent amorphous material, of about 8 for the full beam which had an angular divergence of $\simeq 30$ μrad. In a later measurement, where the angle of incidence was restricted to less than 9 μrad to the axis, the enhancement was shown to be as high as 60 [18]. Furthermore, the enhancement based on the constant-field approximation (CFA) is in very good agreement with the data [19]. The 'Belkacem peak', initially hoped to be a sign of new physics, was later shown to be a result of pile-up of multiple photon emission [20].

A few years after the first confirmation, pair production in strong fields was again addressed by measuring the enhanced pair production yield for photons incident along the $\langle 110 \rangle$ axis of a 1.4 mm Ge crystal cooled to 100 K [21, 22]. A CFA calculation added to the Bethe–Heitler value for the amorphous contribution was shown to fit the data very well and gave compelling evidence for the physical interpretation as a strong-field effect.

More recent studies of strong-field physics in aligned crystal include: (1) pair production [23], where the initially exponentially suppressed coherent contribution becomes dominant as the strong-field regime is entered, (2) the significance of the electron spin, and its associated spin-flip transition in a strong field, in the interpretation of the radiation spectra has been revealed [24], (3) quantum suppression of synchrotron radiation [25] showing the need to correct classical synchrotron radiation formulas once the fields encountered become sufficiently intense, (4) the observation of trident events being enhanced by strong fields [26] and (5) the significance of the radiation reaction phenomenon to describe properly the radiation spectra from electrons in crystals [1], which is the main subject of the present paper. It is worth mentioning that a proposal, based on polarization-sensitive detection in crystalline targets [27], has been published as a viable method to quantify strong-field birefringence.

An introduction to strong-field effects in crystals can be found in these two references [28, 29].

3. Radiation reaction

Radiation reaction is traditionally described by the Lorentz–Abraham–Dirac (LAD) equation in classical electrodynamics [2–4]. The LAD equation, however, has unphysical ('runaway') solutions with, for example, the acceleration of the radiating particle increasing exponentially even if no external field is present. Such features have rendered the LAD equation one of the most controversial equations in physics.

Provided the radiation-reaction force on an electron is much smaller than the Lorentz force in the instantaneous rest frame of the radiating particle, a 'reduction of order' (a perturbation approach) may be applied with the electron's four-acceleration in the radiation-reaction four-force replaced by the Lorentz four-force divided by the electron mass [30]. This results in the Landau–Lifshitz (LL) equation [30],

$$m\frac{\mathrm{d}u^{\mu}}{\mathrm{d}s} = eF^{\mu\nu}u_{\nu} + \frac{2}{3}e^{2}\left[\frac{e}{m}(\partial_{\alpha}F^{\mu\nu})u^{\alpha}u_{\nu} + \frac{e^{2}}{m^{2}}F^{\mu\nu}F_{\nu\alpha}u^{\alpha} + \frac{e^{2}}{m^{2}}(F^{\alpha\nu}u_{\nu})(F_{\alpha\lambda}u^{\lambda})u^{\mu}\right], \tag{1}$$

where $e < 0$ and m denote the electron charge and mass, respectively, $F^{\mu\nu}$ is the external electromagnetic field tensor, u^{μ} is the four-velocity of the electron, and s its proper time in units with $c = 1$. See also [1, equation (1)]. The LL equation is free of the physical inconsistencies of the LAD equation, and it has been shown to feature all the physical solutions of the LAD equation [31].

The dynamics of the particles, and the emitted radiation, is sensitive to the magnitude of the strong-field parameter χ defined as

$$\chi^{2} = (F_{\mu\nu}u^{\nu})^{2}/E_{0}^{2}, \qquad E_{0} = m^{2}/e\hbar, \tag{2}$$

where the critical field assumes a value of $E_0 \simeq 1.32 \times 10^{16}$ V cm^{-1} [32]. For an electron moving in a constant magnetic field, it is essentially $\hbar$ times the characteristic frequency for classical synchrotron radiation divided by the electron energy implying that quantum effects are decisive for χ approaching 1 and above. For an electron or a positron moving in a field that is purely electric (E) in the laboratory and essentially transverse to the direction of motion, as in the case of an aligned crystal, χ reduces to $\gamma E/E_0$, where γ is its Lorentz factor (total energy in units of m).

The ratio of damping force to external force is given by the classical parameter η expressible as

$$\eta = \alpha\gamma^2 E/E_0 = \alpha\gamma\chi, \tag{3}$$

where $\alpha = e^2/\hbar \simeq 1/137$ is the fine-structure constant. For experimental investigations approaching the classical regime, i.e. for $\chi \ll 1$, it is therefore necessary to have large Lorentz-factors, $\gamma \gg 1$, for the magnitude of the radiation damping force to be appreciable in comparison with the Lorentz force, that is, to achieve a non-negligible η.

Strong-field laser experiments offer a very clean interaction compared to crystals, but the technical difficulties of overlapping an electron beam with an ultra short, intense laser pulse, which has an inherent pulse-to-pulse instability, imply that the exact conditions of the interaction are not as well known. Let us relate the parameters defined above to those used in the laser community to compare typical experimental values. Crystalline fields are by nature static and cannot be changed arbitrarily, one can only change the orientation and the target material. Using lasers, instead of crystals, has the advantage of controlling the electric field. The electric field strength of a laser is often described by the gauge- and Lorentz invariant classical non-linearity parameter [33, 34]

$$a_0 = eE/(\omega m) \approx 6.0\ \mu\mathrm{m}^{-1}\lambda\sqrt{2I \times 10^{-20}\ \mathrm{W}^{-1}\ \mathrm{cm}^2}. \tag{4}$$

Here, $\omega = 2\pi/\lambda$ is the characteristic angular frequency of the laser, E denotes its sub-cycle peak electric field strength, and $I = \epsilon_0\langle E^2(t)\rangle_{\mathrm{cycle}}$ is the peak intensity. The classical non-linearity parameter indicates the threshold for which the interaction between a charged particle and the laser becomes non-perturbative (multi-photon absorption from the laser field becomes non-negligible), which happens for $a_0 > 1$ [33]. For a head-on collision between an electron and a laser, we can relate χ, known in the laser community as the quantum non-linearity parameter, and a_0 as

$$\chi = \frac{2\omega m\gamma a_0}{eE_0} \approx 2.9 \times 10^{-5}\gamma\sqrt{2I \times 10^{-20}\ \mathrm{cm}^2\ \mathrm{W}^{-1}}, \tag{5}$$

where half the contribution is due to the magnetic field (B). For a laser we can write the ratio η in terms of a_0 and the laser intensity as

$$\eta = \alpha\frac{2\omega m\gamma^2 a_0}{eE_0} \approx 2.1 \times 10^{-7}\gamma^2\sqrt{2I \times 10^{-20}\ \mathrm{cm}^2\ \mathrm{W}^{-1}}. \tag{6}$$

The initial goal of the upcoming E-320 experiment at SLAC is to operate in the non-perturbative regime with $a_0 \approx 1$ and $\chi \approx 0.15$ with 13 GeV electrons which corresponds to a value $\eta \approx 29$. In this paper, the crystal experiment has a value of $\bar{\chi} \approx 0.06$ for axially aligned 80 GeV electrons, resulting in a value of $\eta \approx 69$. By comparing these two experiments, it is evident that the γ^2 scaling on η benefits the crystal experiments significantly, when studying classical radiation reaction, due to the higher electron energies and lower fields. Another consideration to take into account when comparing the two strong-field experiments, is the spacial extension of the fields. If one seeks to measure the energy loss of, for example, an electron, it generally has to be comparable to the initial energy of the particle. For low values of χ a particle has to spend a significant amount of time in the strong field to lose a measurable amount of energy. Laser experiments achieve strong fields by tightly focusing short laser pulses, meaning that the dimension of the fields are on the micron scale [35, 36]. Crystal fields are on the mm to cm scale and span the entire crystal length which in principle can be arbitrarily long, but in practice are limited by dechanneling from multiple Coulomb scattering on crystal nuclei and valence electrons. On the other hand, as already mentioned, laser-electron interactions are in principle a much cleaner environment for the study of fundamental processes.

In this paper we summarize an experimental verification of the validity of the LL equation by utilizing the strong fields of an aligned single crystal experienced by penetrating high-energy electrons and positrons. The experimental data is compared to simulations based on the LL equation, and for all targets, energies, and crystal orientations tested a remarkable agreement is found between data and simulations. The positron data presented here has been published previously [37] without addressing the LL equation. The electron data has also been published, in [1], where both the positron and electron data were analyzed with the aim of testing the LL equation. While the main conclusions are unchanged, the emphasis in the presentation here is slightly different in view of the expected readership of the special issue. In the experiment 50 GeV positrons cross silicon single crystals in directions close to (110) planes and 40 GeV and 80 GeV electrons cross diamond single crystals in directions close to the $\langle 100\rangle$ axis. Under our experimental conditions we have $\chi \lesssim 0.1$, but values as high as $\chi \simeq 7$ have been achieved using crystals. With η attaining values roughly in the range of 10–100, the radiation-reaction force dominates the dynamics of the particles while χ is on

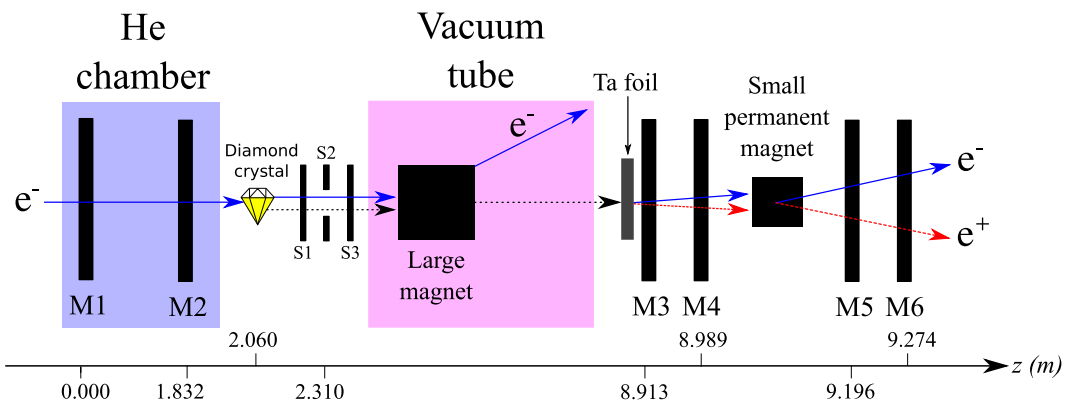

Figure 1. A schematic representation of the experimental setup during the diamond experiment in the H4 beam line in the SPS North Area at CERN. The symbols 'Sj', with $j = 1, 2, 3$, denote the scintillators and the symbols 'Mi', with $i = 1, \ldots, 6$, denote 'Mimosa-26' position sensitive detectors with a resolution of 3.5 μm.

purpose sufficiently small that the influence of quantum effects is moderate. Quantum effects could be further reduced (but never entirely avoided) by using weaker fields, i.e. smaller χ, but the magnitude of the damping force, and thus η, would then decrease and its effect would be difficult to detect. Our experimental conditions therefore provide an ideal approach for testing the applicability of the LL equation.

Previous tests of the LL equation employing intense laser radiation [35, 36] were based on the comparison between the final and the initial energy distribution of ultrarelativistic electrons interacting with a tightly focused terawatt laser, a setup with challenges, for example, large shot-to-shot intensity fluctuations of the laser. An obvious advantage of instead using aligned single crystals is that the electric fields are stationary, stable, and well described.

4. Experiments

The experiments were performed at the H4 beamline of the CERN SPS by the NA63 collaboration. Four silicon single crystals and two diamond single crystals with thicknesses ranging from 1.0 mm to 6.2 mm were used, aligned with the beam along the (110) plane or the $\langle 100 \rangle$ axis, respectively. Findings for the thickest crystal of each material are reported below, the results for all crystals are included in [1]. A schematic of one setup is shown in figure 1.

A thin Ta converter foil was utilized to generate electron–positron pairs from the emitted photons which were subsequently analyzed in a magnetic spectrometer, see figure 1. This procedure gives the single-photon spectrum in the radiation-reaction regime where many photons are emitted by each incoming electron or positron.

For all crystals the background (the radiation with the target removed) was measured and subtracted from the experimental spectra shown. The measured background agrees well with simulations, see also [1].

5. Data analysis and simulations

The experimental spectra presented below are compared to theoretical simulations based on the LL equation as well as to simulations in which the Lorentz force is the sole agent of force on the radiating particle. The reader is referred to [1] for details on these calculations. The classical particle trajectory is determined by the standard Runge–Kutta 45 ordinary differential equation (ODE) solver, where a random change in momentum direction is introduced between every time step due to single collisions with lattice nuclei.

The motion of a charged particle incident at a small angle to a major crystallographic direction is effectively governed by the continuum potential obtained by smearing the atomic charges along the corresponding axis or plane, see [28, 29, 38, 39]. This insight, due to Lindhard *et al* [38], is the key to understanding coherence effects in aligned single crystals. At the energies considered here, the motion is effectively classical. For $\chi \ll 1$ the radiation spectrum may be computed according to standard classical electrodynamics [40]. The only non-negligible quantum effect for the positrons in our experiment is the photon recoil. As shown in a later work by Lindhard [41] the recoil can be taken into account by a simple substitution of the frequency variable in the classical photon number spectrum regardless of the details of

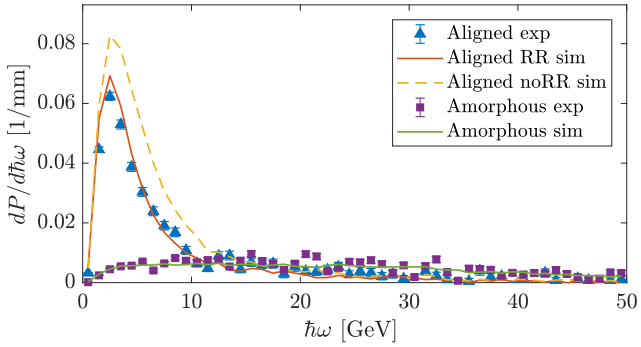

Figure 2. Radiation for 50 GeV positrons passing a 6.2 mm thick silicon crystal aligned along (110) planes. The entry angles to the planes are selected to 0–30 μrad. Experimental data is shown as blue triangles. The theoretical spectra are based on the substitution model. The LL equation simulation ('RR sim') is shown as a red solid line, the Lorentz-force simulation ('noRR sim') is displayed by a yellow dashed line. Purple squares show data for an amorphous/random setting. The simulated amorphous spectrum ('amorphous sim') is shown by a solid green curve. Reprinted figure with permission from [1], Copyright (2020) by the American Physical Society.

the motion of the particle,

$$\omega \to \omega^* = \omega/(1 - \hbar\omega/E). \tag{7}$$

We refer to this as the substitution model. The magnitude of the recoil correction for positrons in our experiment is displayed in figure 1 in [1]. For the electrons, where also the spin affects the radiation spectrum, we apply a formula for the radiation spectrum obtained by Belkacem *et al* [42]. It is based on the semi-classical method by Baier *et al* [43], in which the particle motion is treated classically, whereas the interaction with the radiation field is quantal including both recoil and spin effects. We refer to this as the BCK model. The magnitude of spin effects in radiation for the positrons and electrons in our experiments is also shown in figure 1 in [1]. For the positrons, the substitution and BCK models yield identical results at photon energies where coherence effects due to the crystalline structure are significant, see [1].

Figure 2 shows the radiation recorded for 50 GeV positrons incident on a 6.2 mm thick silicon single crystal with angles in the range 0–30 μrad to the (110) planes. Under these conditions, the average value of χ experienced by the particles is $\bar{\chi} = 0.01$. The selected range in angle of incidence to the planes implies that a substantial fraction of the positrons will be bound to oscillate between a set of neighboring planes (channeling), at least in the first part of the crystal. The experimental data is compared to two simulations, both based on the substitution model. One simulation pertains to the Lorentz force as the sole agent of force (yellow dashed curve), the other pertains to the LL equation (red full-drawn curve). It is evident that the spectrum obtained from the Lorentz force (neglecting the radiation reaction) substantially overshoots the experimental data. The spectrum from the LL equation (including the radiation reaction), on the other hand, closely reproduces the experimental data. For comparison, the figure also displays the spectra measured and simulated for particles incident far from all major crystallographic directions corresponding to the target being amorphous silicon, albeit with the same density as crystalline silicon.

Figure 3 shows the radiation recorded for 80 GeV electrons incident on a 1.5 mm thick diamond crystal with angles to the $\langle 100 \rangle$ axis that are less than the critical angle ψ_1 for channeling, which in this case assumes the value of 35 μrad. At these angles a major part of the electrons will initially be bound to move around a single string of atoms (channeling). The average value $\bar{\chi}$ of the strong-field parameter is 0.06 indicating that quantum effects are modest while more prominent than for the 50 GeV positrons incident near silicon planes. In particular, coherence effects due to the crystal structure extend to photons of higher energy compared to that of the incident particle. This implies that, in addition to photon recoil, also the particle's spin detectably affects the emission process, so we compare the experimental data to simulations based on the BCK model. As in the case of positrons, the simulation in which radiation reaction is neglected strongly overestimates the experimental results. On the other hand, the simulated spectrum based on the LL equation (green dotted line) is substantially lower than the measured spectrum. The reason for this discrepancy is that the radiative energy-loss rate due to classical electrodynamics, which is built into the LL equation, is higher than that obtained by, for instance, the semiclassical BCK approach. But a simplification applies: coherence in the radiation process is only maintained over regions of space connected by the radiation cone. In the considered case, the excursions in angle made by the electrons interacting with the continuum strings are much larger than the opening angle of this cone. Hence coherence is only maintained over fragments of the path corresponding to small variations in the distance to the atomic strings, and hence, to small variations in the encountered field strengths. In other words, the radiation may be

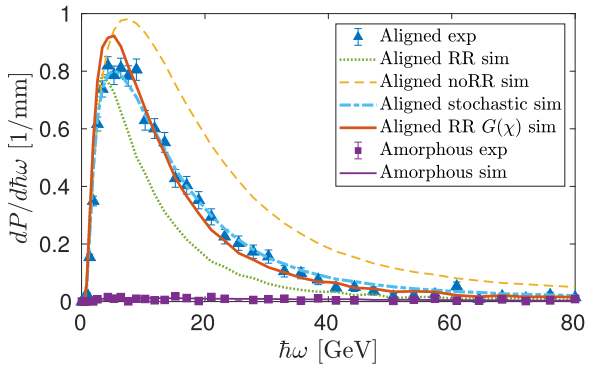

Figure 3. Radiation for 80 GeV electrons traversing a 1.5 mm thick diamond crystal aligned to the ⟨100⟩ axis. The entry angles to the axis are less than Lindhard's critical angle for channeling, $\psi_1 = 35$ μrad. Symbols for data and the simulation neglecting radiation reaction are as in figure 2. The theoretical spectrum calculated using the BCK model and based on the LL equation ('RR sim') is shown as a green dotted line while the spectrum based on the same model and equation but including the $G(\chi)$ correction ('RR $G(\chi)$ sim') is shown as a red solid line. The dashed-dotted blue line shows the spectrum calculated using the BCK model in the stochastic scheme [1] ('stochastic sim') and the simulated amorphous spectrum ('amorphous sim') is shown as a solid purple line. Reprinted figure with permission from [1], Copyright (2020) by the American Physical Society.

computed as if the field were constant locally, see [1] and references therein. The ratio of the quantum and the classical radiated energy in a constant field may be parametrized as [25, 43]

$$G(\chi) = \left[1 + 4.8(1+\chi)\ln(1+1.7\chi) + 2.44\chi^2\right]^{-2/3}. \tag{8}$$

When this reduction is included in an approximate manner by multiplying the damping force in the LL equation by $G(\chi)$, it produces the red simulation curve shown in figure 3 that essentially reproduces the experimental spectrum. The result of a quantum simulation, the so-called stochastic scheme, is shown by a blue dashed-dotted line. It does not involve the classical LL equation but instead emission of quanta of finite energy. In a given segment the photon emission is a statistical process governed by probabilities computed in the semiclassical BCK approach, see [1] for details. Except for a narrow region around the spectral maximum, where the quantum simulation is slightly superior, there is not much difference between our simulation based on the LL equation and the quantum simulation.

Since the energy losses are moderate for the positrons in the planar channeling regime, it could be expected that spectra obtained neglecting radiation-reaction effects would be roughly adequate, but the experiments and simulations clearly show that it is not the case. The simulations without radiation reaction overestimate the emitted radiation significantly. The electrons in the axial channeling regime, on the other hand, experience large energy losses as they traverse the crystal. Here exclusion of the G-factor implies an overestimate of the damping force and, in turn, an underestimate of electron energy already after traversing a small part of the crystal, and hence of the emitted radiation intensity in the later parts of the crystal.

As seen in figures 2 and 3, the photon emission spectra have features that cannot be explained by using only the Lorentz force to calculate the particle trajectories. Moreover, when the radiation reaction is included in the simulations, the agreement between theory and data is remarkably good. Despite this, there remains a discrepancy between the energy loss calculated from the LL equation and calculated by integrating the radiation spectrum. This discrepancy is due to the quantum corrections introduced in the radiation process. The positrons in figure 2 lose 17% of their incoming energy by integrating the radiation spectrum and 20% of their incoming energy according to the LL equation, corresponding to an excess of the loss according to the LL equation over the spectrum energy loss by 19%. Due to the stronger fields encountered, the discrepancy is *a priori* larger in the axial channeling regime as in figure 3 where the electrons lose more than half of their initial energy. However, the inclusion of the G-factor on the damping force in the LL equation reduces the ratio of the radiation energy loss resulting from the LL equation to the spectrum energy loss to just 1.07. This modest difference of 7% may be taken as an indication of the quality of the procedure of including the G-factor on the damping force as well as of the close proximity to a scenario with photon production in a (locally) constant field.

6. Conclusion

The Lorentz force has been shown to be insufficient in describing the dynamics and resulting radiation spectra in our crystal-based strong-field experiments. This deficiency is remedied by theoretical predictions

resting on the LL equation, when adjusted through the substitution model accounting for the photon recoil in the radiation spectra from planar channeled 50 GeV positrons. Remarkable agreement with the experimental results is obtained. Similarly, and equally convincing, for axially channeled 80 GeV electrons, when accounting for photon recoil, particle spin, and applying a quantum correction to the radiation intensity, the LL equation nicely reproduces the experimental spectra.

These agreements, obtained in all the cases we have tested, provide compelling experimental evidence that the LL equation is essential and accurate in describing radiation under large accelerations, where the back-action becomes the dominant force. The LL equation has thus been verified to describe the classical phenomenon of radiation reaction to a high degree of precision.

Acknowledgments

We are grateful for the assistance provided by T N Wistisen in designing and executing the experiments. We further acknowledge the superb technical help and expertise from Per Bluhme Christensen, Erik Loft Larsen and Frank Daugaard (AU) in setting up the experiment and data acquisition. The numerical results presented in this work were partly obtained at the Centre for Scientific Computing Aarhus (CSCAA) and with support from Nvidia's GPU grant program. This work was partially supported by the U.S. National Science Foundation (Grant Nos. PHY-1535696 and PHY-2012549) and the National Instrument Center for CERN in Denmark.

Data availability statement

The data that support the findings of this study are available from the authors upon reasonable request.

ORCID iDs

C F Nielsen https://orcid.org/0000-0002-8763-780X
J B Justesen https://orcid.org/0000-0003-2525-6793
U I Uggerhøj https://orcid.org/0000-0002-8229-1512
R Holtzapple https://orcid.org/0000-0003-2726-1131

References

[1] Nielsen C F, Justesen J B, Sørensen A H, Uggerhøj U I and Holtzapple R (CERN NA63 Collaboration) 2020 *Phys. Rev.* D **102** 052004
[2] Abraham M 1905 *Theorie der Elektrizität* (Leipzig: Teubner)
[3] Lorentz H A 1909 *The Theory of Electrons* (Leipzig: Teubner)
[4] Dirac P A M 1938 *Proc. R. Soc.* A **167** 148
[5] Barut A 1980 *Electrodynamics and Classical Theory of Fields and Particles* (New York: Dover)
[6] Rohrlich F 2007 *Classical Charged Particles* (Singapore: World Scientific)
[7] Baryshevskii V G 1978 *Proc. 15th Winter School of LIYaF* vol 158 (Leningrad)
[8] Baryshevskii V G 1981 *Vestn. Akad. Nauk. Bueloruss. SSR* **4** 104
[9] Baryshevskii V G and Thikhomirov V V 1982 *Sov. J. Nucl. Phys.* **36** 408
[10] Baryshevskii V G and Thikhomirov V V 1982 *Phys. Lett.* A **90** 153
[11] Kimball J C, Cue N, Roth L M and Marsh B B 1983 *Phys. Rev. Lett.* **50** 950
[12] Belkacem A *et al* 1984 *Phys. Rev. Lett.* **53** 2371
[13] Cue N, Marsh B B, Pisharody M, Sun C R, Bian Z H, Lin I C, Park H, Gearhart R A and Murray J J 1984 *Phys. Rev. Lett.* **53** 972
[14] Belkacem A *et al* 1985 *Phys. Rev. Lett.* **54** 2667
[15] Kimball J C and Cue N 1984 *Phys. Rev. Lett.* **52** 1747
[16] Kimball J C and Cue N 1985 *Phys. Rep.* **125** 69
[17] Belkacem A *et al* 1986 *Phys. Lett.* B **177** 211
[18] Medenwaldt R *et al* 1989 *Phys. Rev. Lett.* **63** 2827
[19] Baier V N, Katkov V M and Strakhovenko V M 1991 *Nucl. Instrum. Methods Phys. Res.* B **62** 213
[20] Medenwaldt R *et al* 1990 *Phys. Lett.* B **242** 517
[21] Belkacem A *et al* 1986 *Nucl. Instrum. Methods Phys. Res.* B **13** 9
[22] Belkacem A *et al* 1987 *Phys. Rev. Lett.* **58** 1196
[23] Moore R *et al* 1996 *Nucl. Instrum. Methods Phys. Res.* B **119** 149
[24] Kirsebom K, Mikkelsen U, Uggerhøj E, Elsener K, Ballestrero S, Sona P and Vilakazi Z Z 2001 *Phys. Rev. Lett.* **87** 054801
[25] Andersen K K *et al* (CERN NA63) 2012 *Phys. Rev.* D **86** 072001
[26] Esberg J *et al* (CERN NA63) 2010 *Phys. Rev.* D **82** 072002
[27] Wistisen T N and Uggerhøj U I 2013 *Phys. Rev.* D **88** 053009
[28] Sørensen A H 1996 *Nucl. Instrum. Methods Phys. Res.* B **119** 2
[29] Uggerhøj U I 2005 *Rev. Mod. Phys.* **77** 1131

[30] Landau L D and Lifshitz E M 1975 *The Classical Theory of Fields* (Amsterdam: Elsevier)
[31] Spohn H 2000 *Europhys. Lett.* **50** 287
[32] Berestetskii V B, Lifshitz E M and Pitaevskii L P 1989 *Quantum Electrodynamics* (Oxford: Pergamon)
[33] Ritus V I 1985 *J. Sov. Laser Res.* **6** 497
[34] Umstadter D 2003 *J. Phys. D: Appl. Phys.* **36** R151
[35] Poder K *et al* 2018 *Phys. Rev.* X **8** 031004
[36] Cole J M *et al* 2018 *Phys. Rev.* X **8** 011020
[37] Wistisen T N, Di Piazza A, Nielsen C F, Sørensen A H and Uggerhøj U I (CERN NA63) 2019 *Phys. Rev. Res.* **1** 033014
[38] Lindhard J 1965 *Kong. Danske Vidensk. Selsk, Mat.-Fys. Medd* **34** 1
[39] Andersen J U 2018 Notes on channeling *Lecture Notes* (Aarhus University) https://phys.au.dk/publikationer/lecture-notes/
[40] Jackson J D 1975 *Classical Electrodynamics* (New York: Wiley)
[41] Lindhard J 1991 *Phys. Rev.* A **43** 6032
[42] Belkacem A, Cue N and Kimball J C 1985 *Phys. Lett.* A **111** 86
[43] Baier V N, Katkov V M and Strakhovenko V M 1998 *Electromagnetic Processes at High Energies in Oriented Single Crystals* (Singapore: World Scientific) p 554